DOI: 10.1002/asia.200800195

Advances and Prospects of Gold Nanorods

Da-Peng Yang and Da-Xiang Cui*[a]

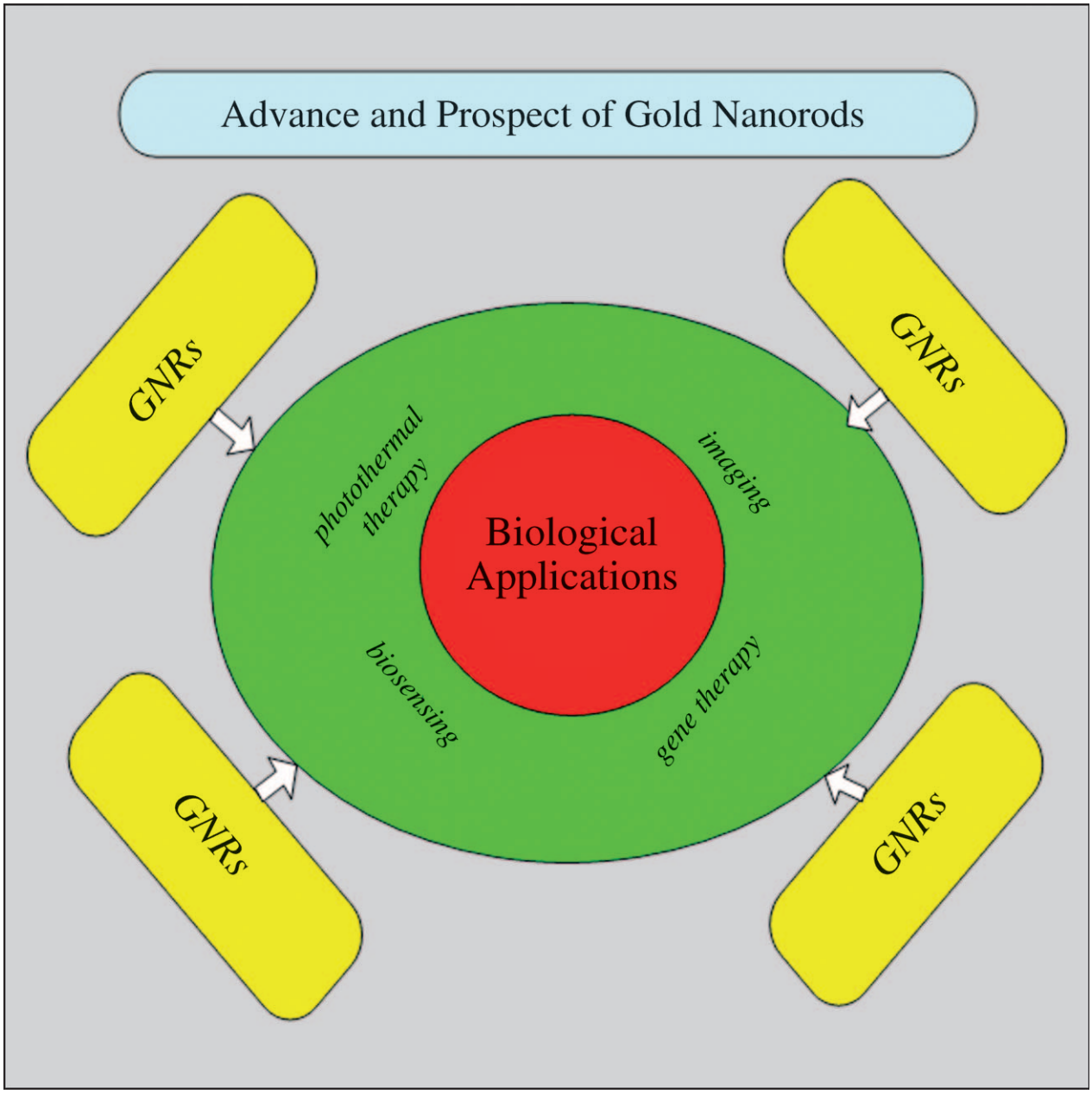

Abstract: With the development of nanotechnology, many novel nanomaterials with unique properties such as magnetic, electronics, and photonics are increasingly being exploited. Gold nanorods, which are rod-shaped nanomaterials, show powerful potential in biological/biomedical fields, especially photothermal therapy, biosensing, imaging, and gene delivery for the treatment of cancer. Many scientific groups have shown strong interests in gold nanorods and have attempted to push them towards possible clinical applications. However, owing to the quantum-size effects of nanomaterials, people have also raised some concerns about the potential toxicity hazards. Therefore, it is becoming urgent to study and exploit the biological effects of gold nanorods for benefit in the near future.

Keywords: biosensors · gene delivery · gold nanorods · molecular imaging · photothermal therapy

1. Introduction

Gold nanords (GNRs), as one important member of the noble-metal nanoparticles(Au, Ag, Cu),[1–3] are attracting intensive scientific interest for their unique properties and potential applications such as photothermal therapy,[4–6] biosensing,[7–9] molecular imaging,[10–12] and gene delivery[13,14] for cancer treatment. Owing to surface plasmon resonance,[15,16] gold nanorods show greatly enhanced absorption and Rayleigh scattering of light. In a sense, GNRs are elongated gold nanoparticles with unique optical properties depending on their size and shape.[17,18] However, unlike spherical gold nanoparticles, GNRs possess two absorption bands owing to the surface plasmon collective oscillation of free electrons.[19,20] One is called the transverse plasmon band, relating to the absorption and scattering of light along the short axis of rods, located in the visible region at about 520 nm; the other is called the longitudinal plasmon band, relating to the absorption and scattering of light along the long axis of the rods, located in the near-infrared (NIR) region of the electromagnetic spectrum, which is tunable by changing certain aspects of GNRs.[21] It has been thought that biological tissues are relatively transparent in the NIR[22] region, where there are many exciting applications for photodynamic[23] and photothermal therapy of cancer.[24,25] Based on this, GNRs are extremely attractive candidates with essential properties as optical sensors for biological and medical applications, for example, photothermal therapy,[6,26] optical imaging,[21] and biosensing.[9] Moreover, GNRs can greatly enhance the surface Raman scattering of adsorbed molecules,[27] and therefore can act as the substrate of Raman probe design.[28] Although GNRs display promising prospects, there are still some concerns on their synthesis,[29,30] surface modifications,[18] biocompatibility and toxicity,[31] and so on. Herein, we review the main progresses made over the past few years in the synthesis, surface modification, molecular assembly, and biological effects of gold nanorods, exploring their application prospects in photothermal therapy, biosensing, molecular imaging, and gene delivery, with the aim of stimulating a broader attention to GNRs and improving the development of GNR-based nanotechnology.

[a] Dr. D.-P. Yang, D.-X. Cui
Department of Bio-Nano Science and Engineering
National Key Laboratory of Nano/Micro Fabrication Technology
Key Laboratory for Thin Film and Microfabrication of Ministry of Education
Institute of Micro and Nano Science and Technology
Shanghai Jiao Tong University
Shanghai 200030
Fax: (+86) 21-34206886
E-mail: dxcui@sjtu.eud.cn

2. Synthesis and Optical Properties

There is wide interest in synthesizing different shapes of gold nanomaterials.[32] So far, gold nanomaterials such as gold nanospheres,[33] gold nanobelts,[34] gold nanocages,[35,36] gold nanoprisms,[37] gold nanostars,[38,39] and gold nanorods[30] have been successfully fabricated, and their formation mechanism and important physical and chemical properties are being investigated.

Among these gold nanomaterials, GNRs have received more attention, and a lot of references are associated with them. In comparison with other shapes of gold nanomaterials, GNRs possess several advantages: different synthetic methods can be chosen,[18] mild reaction conditions can be used,[40] high yields and narrow site distribution[41,42] can be gained through judicious choice of experimental parameters.

Furthermore, GNRs have a higher efficiency of light absorption at their longitudinal plasmon resonance site than any other known nanomaterials, including gold nanoshells.[43,44]

To date, the main methods to synthesize GNRs include porous aluminum template methods,[45] electrochemical methods,[45] photochemical methods,[46] and the seed-mediated growth method.[47] Of all these methods, the seed-mediated growth method has the longest history, which dates back to the 1920s,[18] and is especially appealing and widely adopted because it is very simple and flexible in fabricating different aspect ratios of GNRs and keeping a relatively high yield. Generally, the seed-mediated growth method includes two steps: synthesis of seeds and the growth of seeds.[40] The former is done by using a strong reducing agent to reduce a metal salt solution in aqueous medium so as to get a certain size of spherical gold nanoparticles, which are defined as gold seeds. After the gold seeds are formed, the next step is to add them into the surfactant, which acts as a soft template to direct seed growth. During the growth, another weak reducing agent is necessary to guarantee the reduction of gold salt. To get a high yield of tailored GNRs by this method, several parameters such as the seeds themselves[30] (size and aging time), use of $AgNO_3$,[17,41] use of cetyltrimethylammonium bromide (CTAB),[48] pH,[49] temperature,[50] among others must be carefully considered before preparation because the formation mechanism of GNRs is very complicated; a slight variation will affect the size and shape of the GNRs. The Murphy group[51,52] performed some pioneering work on the seed-mediated growth of GNRs. The formation mechanism of GNRs has so far still not been well clarified,[27,47,53] though Perez-Juste et al.[18,53] provided an excellent overview to discuss this problem in detail.

Gold nanoparticles show a strong absorption band in the visible region owing to the collective oscillations of metal conduction band electrons in strong resonance with visible frequencies of light, which is called surface plasmon resonance (SPR).[54] There are several parameters to influence the SPR frequency. For example, the size and shape of the metal nanoparicles, surface charges, dielectric constant of the surrounding medium, and so on.[55,56] Upon changing the shape of gold nanoparticles from spheres to rods, the SPR spectrum exhibits two absorption bands: a weaker short-wavelength in the visible region owing to the transverse electronic oscillation and a stronger long-wavelength band in the NIR region owing to the longitudinal oscillation of electrons. The aspect ratio of GNRs can markedly affect their absorption spectra.[19] In the same vein, increasing the aspect ratio can lead to longitudinal SPR absorption band red-shifts. This interesting phenomenon will benefit us enormously in practical applications.

3. Surface Modifications

To obtain a high yield of GNRs, CTAB, an important cationic surfactant, is frequently used, which acts not only as an inducing agent but also a capping agent.[18] CTAB forms the bilayer structure on the surface of GNRs, whereby the trimethylammonium head groups of the first monolayer are facing the surface of the GNRs, while the absorbed second layer of CTAB extends outside the groups with positive charges through van der Waals interactions between the surfactant tails.[57] The CTAB molecule has a long alkyl chain, which makes it difficult to further modify GNRs in the presence of abundant CTAB.[58] Furthermore, removing excess CTAB will cause GNRs to undergo irreversible aggregation.[59] Therefore, it is imperative to implement surface modifications before further biological applications. For exploring applications, there are three kinds of molecules mainly used for the surface modifications of GNRs: small-molecule compounds, polymers, and inorganic silica.

Abstract in Chinese:

金纳米棒，作为一类新兴的贵金属纳米材料，拥有独特的光学性质，在电子、光子、化学和生物学领域有着广泛的用途。尤其是最近几年，越来越多的研究者正推动着其向生物学领域的快速发展。本文对金纳米棒的合成、表面修饰、分子组装和生物学效应等方面进行了综述，重点介绍了在光热治疗、生物感知、成像和基因传送方面的应用前景，目的是尽早实现该材料的临床应用。

Daxiang Cui *received his PhD degree from Xi'an Fourth Military Medical University in 1998. He joined the Max Planck Institute for Metals Research as a Visiting Scientist in 2001 and was promoted to Scientific Staff in 2002. He became a professor in the Institute of Micro-Nano Science and Technology, Shanghai Jiao Tong University in 2004. He is also a guest professor of Waseda University from 2007. His research interests mainly focus on biological effects and bi-safety of nanomaterials, nanoscale diagnosis and therapy technologies, biochips, and the structure and function of gene and protein.*

Dapeng Yang *received a Master of Science degree in Biology from the Shandong University of Technology in 2004. He is currently a PhD student of Shanghai Jiao Tong University. His primary interests are in the preparation and application of nanomaterials.*

Yamada et al.[59] demonstrated an extraction technique using phosphatidylcholine (PC) to modify GNRs, in which CTAB was successfully extracted into a chloroform phase while PC adsorbed onto the GNRs. Zeta potential indicated that some CTAB molecules were still retained on the face of the GNRs, but the cytotoxicity was reduced to a negligible degree. For further biological applications, both long-term stability and facile modification methods are essential. Instead of partial modification, Irudayaraj et al.[58] reported a chemical method to replace CTAB on the surface of GNRs. They synthesized two types of biocompatible small organothiols, one positively charged and the other negatively charged. Both compounds have SH groups, which show a strong affinity for gold atoms. In this approach, they emphasized that a series of factors are pivotal to the successful activation of GNRs. It seems that CTAB is prone to bind tightly onto the Au surface so that small-molecule compounds cannot easily replace them. In comparison to polymer modifications, small linker molecules are more available for biosensing applications. Since the plasmonic electromagnetic field around GNRs decays exponentially from the surface, polymer coating creates a thicker layer which is less sensitive to surface-binding events than small-molecule counterparts.

Polymers are very efficient and widely used mediums for surface modifications. Murphy and co-workers[60] first suggested a layer-by-layer (LbL) approach to modify the entire surface of GNRs by electrostatic self-assembly, in which the positively charged CTAB facilitated absorption of an anion polyelectrolyte, poly(sodium-4-styrenesulfonate) (PSS). Subsequently, a cationic polyelectrolyte, poly(diallyldimethylammonium chloride) (PDADMAC) was further utilized. The process could alternately be repeated to deposit polyelectrolyte multilayers. Boyes and co-workers[61] provided another technique called reversible addition-fragmentation chain transfer (RAFT) to modify GNRs with different polymers. RAFT is a versatile controlled "living" free-radical polymerization technique which has played a key role in polymers synthesis. In comparison to the LbL method, several advantages are evident: stronger binding to the substrate surface, control over the thickness, and more than just polyelectrolyte materials. Using this technique, they modified the surface of GNRs with both hydrophilic polymers poly(2-(dimethylamino)ethyl methacrylate) (PDMAEMA), poly(acrylic acid) (PAA), and the hydrophobic polymer polystyrene (PS). The thickness of polymers attached to the surface of GNRs was tunable from 3 nm to 14 nm. The maximum shifts of both PDMAEMA and PS corresponded well with the TEM results. But, for PAA, it caused aggregation. Niidome et al.[62] added MPEG-SH into the GNR solution stabilized by CTAB to achieve PEG modification. PEG-modified GNRs reduced cytotoxicity significantly and showed a stealth character in vivo. PEG-modified GNRs were assumed to be well suited for biomedical applications. In addition, some groups also utilized PVP,[63] lipids,[64] copolymer,[65] bovine serum albumin (BSA), and polyethlenimine (PEI)[66] to modify the surface of GNRs.

Since great efforts were made on silica-coated works by the Mulvaney,[67] Philipse,[68] and Iler[69] groups in the past decades, recently the inorganic silica-coating method has become of increasing interest for the surface modification of nanomaterials, for example, of Au,[70] Fe_3O_4,[71] Ag,[72] and quantum dots.[73] There are several main reasons for this. Firstly, silica surface chemistry has been well established; one can easily covalently introduce functional groups to the silica surface. Secondly, coating a shell of pure transparent silica has little influence on the physical properties of nanomaterials including optical, magnetic, and catalytic performances. More importantly, silica coating enhanced the colloidal stability. Murphy et al.[74] successfully reported the use of γ-methacryloxypropyltrimethoxysilane(MPS) to coat the high-aspect-ratio GNRs (aspect ratio 13). However, their method was not available specifically for short-aspect-ratio GNRs which often exhibited poor reproducibility and particle aggregation. Later, Perez-Juste et al.[63] brought forward a new silica-coating profile to overcome this defect using a combination of the LbL technique and hydrolysis and condensation of tetraethoxy silane (TEOS), leading to a homogeneous coating (Figure 1).

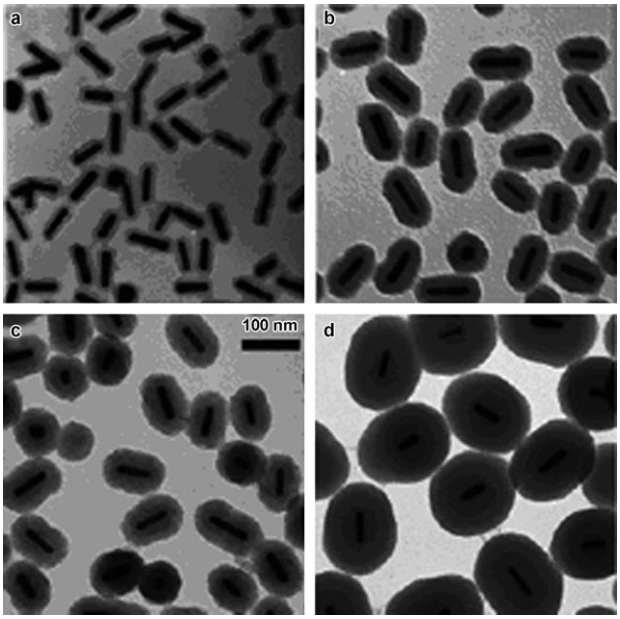

Figure 1. TEM images of GNRs with controlled silica shell thickness. From (a) to (d), the shell thickness gradually increases. Reprinted with permission from reference [63].

A silica shell not only can control the dipolar interactions between GNRs, but also can enhance the versatility of the particles. Ma and co-workers[75] prepared the Au_{rod}/SiO_2 composites through an improved Stöber method. The uniform shell thickness was about 9 nm. To avoid the nucleation of free silica in solution, they adopted vortex mixing rather than mechanical mixing and magnetic stirring. This is because vortex mixing can afford more homogeneous mixing. Here, it must be pointed out that obtaining a de-

fined homogeneous layer of silica is not as easy as described in most papers; one must be cautious about operation and dosage during the process of coating.

4. Molecular Assembly

Assembling one or more molecular entities may produce novel physical properties which are very useful in nanoscale electron device fabrication. GNRs with unique optical properties play an important role in nanomaterial assembly and are attracting more and more attention. Electrostatic, hydrophilic–hydrophobic, and specific interactions (antigen–antibody, oligonucleotides, biotin–streptavidin, aptamer–protein) are often involved in the GNR assembly.[76]

El-Sayed et al.[77] showed that simple solvent evaporation results in the organization of 1D, 2D, and 3D structures of GNRs. Zubarev and co-workers[78] described a simple method to spontaneously assemble hybrid gold–polymer core–shell nanorods into ringlike arrays (Figure 2).

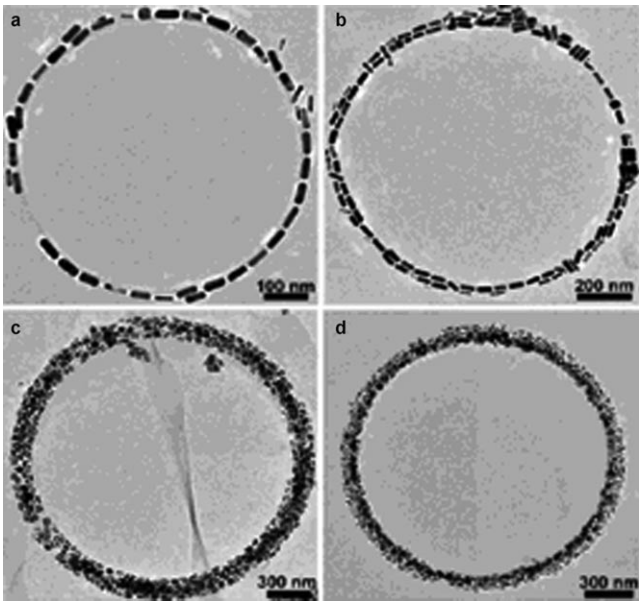

Figure 2. a–d) TEM images of rings formed by GNR-$(PS)_n$ from a solution of CH_2Cl_2 (1 mg mL^{-1}). Reprinted with permission from reference [78].

The mechanism of developing ringlike structure is as follows: Polystyrene (PS) chains are covalently attached to GNRs, then the hybrid core–shell materials are dissolved into CH_2Cl_2 solvent. When highly volatile CH_2Cl_2 is evaporated quickly and cooled so that its surface is below the dew point, the numerous water droplets of air start to condense and drop onto the substrate and are surrounded by the CH_2Cl_2 solution of GNRs/PS. The increasing water droplets gather to develop a template. Since GNRs/PS are highly soluble in CH_2Cl_2, they remain in the solution until the last portion of CH_2Cl_2 is concentrated around the impervious walls of the water droplets. After being dried at the lower temperature, the sample starts to return to room temperature, thus causing evaporation of the water templates and development of ringlike arrays of the GNRs.

Some research groups have utilized the well-known biotin–streptavidin specific recognition mechanism to assemble GNRs. Murphy and co-workers[79] reported that short-aspect-ratio GNRs treated with biotin were assembled preferentially in an end-to-end fashion when mixed with streptavidin (Figure 3). This is because biotin disulfide failed to replace all CTAB, and thus biotin preferentially binds to the faces at the ends of the rods.[76] Then, they examined the effect of biotin–streptavidin on the long gold nanorods.[80] Firstly, GNRs were uniformly biotinylated. Subsequently, streptavidin was added into the biotinylated GNRs, leading to nanorod aggregation. This phenomenon revealed that the GNRs preferentially underwent side-to-side assembly when forming 3D aggregates. Otherwise, through oligonucleotide matching and antigen–antibody recognition, The Tan group[76] and our group[81] discovered that GNRs preferentially assembled themselves in an end-to-end fashion in the presence of CTAB (Figure 4). These assembled GNRs can reach as long as the micrometer scale through control of the concentrations.

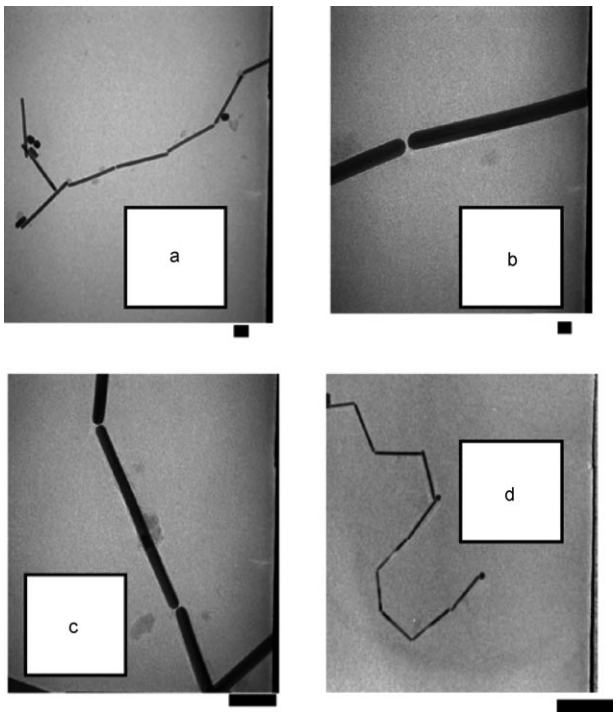

Figure 3. TEM imagines of GNRs, surface-derivatized with either biotin disulfide, after addition of streptavidin. Scale bars from (a) to (d): 100 nm, 20 nm, 100 nm, and 500 nm, respectively. Reprinted with permission from reference [79].

Several investigators[82–85] also showed that cysteine and/or glutathione as molecular bridges possessed the same capability to assemble GNRs in preferential end-to-end fashion.

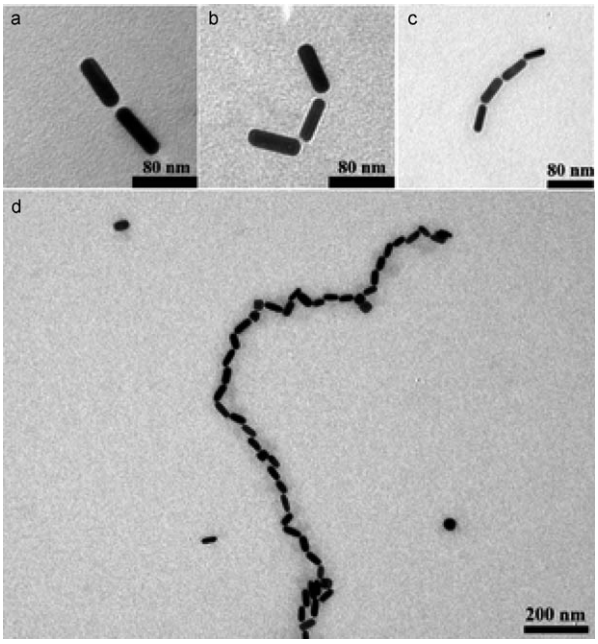

Figure 4. TEM images of a) di-, b) tri-, c) tetragold nanorods assembly. The antimouse IgG provides an anchoring site at the end surface of nanorod and interacts with mouse IgG for assembly. d) GNRs were assembled into successive chains by stepwise increasing concentration of mouse IgG. Reprinted with permission from reference [76].

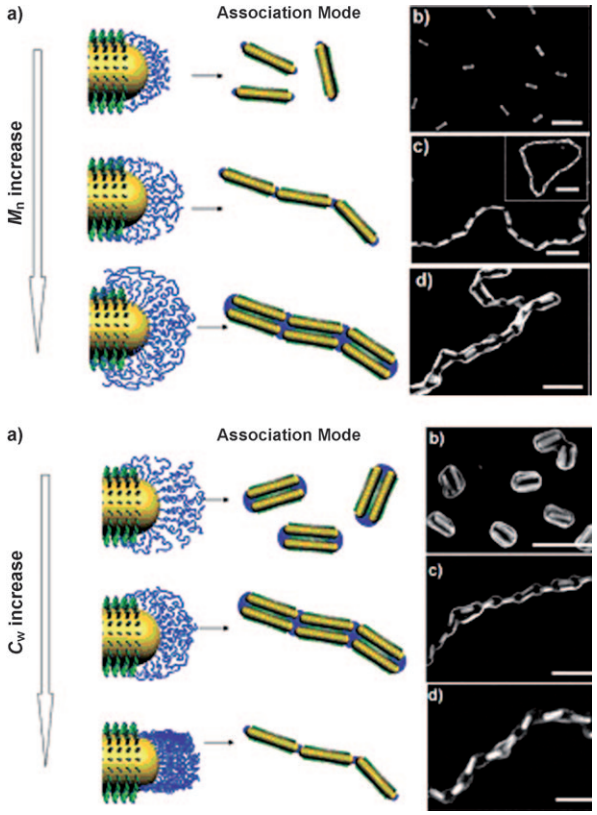

Figure 5. Top: a) Schematic illustrations of the relative location of PS molecules with varying molecular weight (left), and illustrations of the self-assembled structures of triblocks (right). b–d) SEM images of the self-assembled structures of triblocks carrying different molecular weights. Scale bars: 100 nm. Bottom: a) Schematic illustrations of the relative location of PS molecules with varying water content (left), and illustrations of the self-assembled structures of triblocks with 50 K PS (right). b–d) SEM images of corresponding assembled structures of triblocks with 50 K PS in different water/DMF mixture. Scale bars: 100 nm. Reprinted with permission from reference [92].

Electrostatic interaction[86,87] is in general a facile method to carry out nanomaterial assembly. Liz-Marzan et al.[88] aligned GNRs along multiwalled carbon nanotubes to develop stringlike structures through static interactions. Murphy et al.[89] immobilized GNRs onto 2D surfaces through electrostatic interaction between the positively charged CTAB and negatively charged SAMs (self-assembled monolayers of 16-mercaptohexadecanoic acid). Using the same principle, our group[90] carried out formation of DNA-templated ordered arrays of GNRs in one and two dimensions. Before this, Mann et al.[91] reported that GNRs organized into anisotropic 3D aggregates under the drive of DNA hybridization. More recently, Kumacheva and co-workers[92] reported the assembly of GNRs end-terminated with multiple polymer arms (pom-poms). Interestingly, they showed that through changing two anticorrelating parameters, the molecular weight of the polymer tethered to GNR end and the fraction of water in the system, shape transitions can be controlled (Figure 5).

In summary, 1D, 2D, and 3D assembly of GNRs can produce some interesting structures which are useful in the design of nanodevices. Exploration on the mechanism of assembly of GNRs will enhance the understanding of molecule assembly.

5. Biological Effects

As-prepared GNRs contain a large amount of free CTAB molecules in the solution, which exhibit high cytotoxicity.[62,93] As mentioned previously, CTAB molecules develop bilayers on GNRs and are dynamic. That is to say, the solution always contains free CTAB from rod surfaces even if one can remove all of unbound CTAB from the original solution.[58] Furthermore, repeated centrifugation results in irreversible aggregation of the GNRs. It is now considered that CTAB-bound GNRs are nontoxic; the cytotoxicity is attributed to free CTAB.[94] Therefore, the existence of CTAB and following surface modification raise big concerns. Wyatt and co-workers[94] studied the uptake and acute toxicity to human leukemia cells of several different diameters of spherical gold nanoparticles with a variety of surface modifiers. Their results show that nanoparticles themselves are not necessarily detrimental to cellular function. However, more and more evidence shows that the uptake and toxicity of nanomaterials depend on size, shape, and surface modifications (charges, functional species).[95] Yamada[59] et al. used PC-passivated GNRs to suppress the desorption of CTAB and showed lower cytotoxicity than the twice-centrifuged CTAB-capped GNRs. Nevertheless, PC-modified GNRs are

unstable and do not facilitate further biofunctionalization. Chan et al.[96] investigated the uptake of transferrin-coated gold nanoparticles of different sizes and shapes in fibroblast cells, ovarian cancer cells, and brain tumor cells. The results showed that transferrin-coated gold nanopartilces were taken up by a clathrin-mediated endocytosis pathway, while GNRs had a lower uptake than spherical gold nanoparticles. With increasing aspect ratio, the rates of uptake were slower. The fraction of rod-shaped nanoparticle exocytosis was higher than that of spherical-shape nanoparticles. Recently, this group has systemically assessed PE-coated GNR uptake, toxicity, and gene expression.[31] Their results show that a series of factors (surface functional groups, charge, and PEs) may affect the uptake of GNRs. Gene expression analysis confirms that indicators of cell stress are not significantly up- or down-regulated even if large quantities of GNR uptake occur. Among 10000 genes assessed, only 35 appeared down-regulated as shown[31] (see the list of genes in Table 1). Therefore, GNRs are suited for biological applications.

6. Biological Application Prospects

6.1. Photothermal Effects

GNRs are a novel photothermal agent that can absorb NIR light efficiently to transfer into heat to destroy biological tissues.[97] Therefore, they are efficient exogenous agents to the therapy of cancer.[5] In particular, targeted GNRs[98] are mandatory so as to avoid the photothermal ablation to health tissues resulting from an unspecific uptake. El-Sayed et al.[26] conjugated GNRs to anti-EGFR monoclonal antibodies (many solid tumors overexpress EGFR) and incubated them in a nonmalignant epithelial cell line and two malignant oral epithelial cell lines. The anti-EGFR/GNRs themselves were not cytotoxic and destroyed the tumor cells without harming healthy cells after light irradiation (Figure 6).

The important finding is that the threshold energy of killing cancer cells is lower than other core–shell particles. Wei and co-workers[99] investigated photothermal effects of folate-conjugated GNRs to KB cells. With the help of real-time TPL microscopy, they found that photothermolysis of KB cells was particularly effective when folate-GNRs were localized on the cell membrane following fs-pulsed excitation (Figure 7). Folate-GNR-mediated cavitation disrupted membrane integrity, leading to cell death. Their results are quite distinct from traditional assumptions of nanoparticle-mediated hyperthermia which are only based on systemic temperature changes. Besides aiming at cancer cells with photothermal effects of targeted GNRs, two groups also found some interesting applications in fighting against pathogenic bacteria[100] and parasites.[101] GNR photothermal therapy may also open a new avenue to treating infections diseases.

6.2. Molecular Imaging

In modern medicine, multimodal imaging[102] is increasingly pursued so that doctors can predict and diagnose diseases more accurately. No single molecule can play this role.

Table 1. Names of genes exhibiting significant change following treatment with GNRs. Reproduced with permission from reference [31].

Accession number	UG[a]	Fold change	Gene name
R80235	Hs.567303	5.33	Mdm2, transformed 3T3 cell double minute 2, p53 binding protein (mouse)
AA865265	Hs.437060	2.40	Cytochrome *c*, somatic
R32833	Hs.487510	8.18	Carbohydrate (*N*-acetylglucosamine 6-O) sulfotransferase 6
N20989	Hs.165859	4.77	Anthrax toxin receptor 1
R06452	Hs.642603	1.77	Vasodilator-stimulated phosphoprotein
R25583	Hs.533262	2.60	Anaphase-promoting complex subunit 2
AA421819	Hs.171054	1.77	Cadherin 6, type 2, K-cadherin (fetal kidney)
H94063	Hs.44235	4.55	Chromosome 13 open reading frame 1
CD300603	Hs.501149	1.87	PDZ domain containing 8
AA931818	Hs.602357	3.66	Transcribed locus
AA028927	Hs.460109	1.55	Myosin, heavy polypeptide 11, smooth muscle
T78481	Hs.260041	1.72	CAS1 domain containing 1
AA456299	Hs.444558	1.48	KH domain containing, RNA binding, signal transduction associated 3
AA031420	Hs.244139	1.40	Fas (TNF receptor superfamily, member 6)
AA001870	Hs.598312	1.51	Phosphoglucomutase 3
W68280	Hs.234521	2.14	Mitogen-activated protein kinase-activated protein kinase 3
W91887	Hs.403917	2.86	FERM, RhoGEF (ARHGEF), and pleckstrin domain protein 1 (chondrocyte-derived)
R99627	Hs.486084	2.11	Chromosome 6 open reading frame 203
N64604	Hs.97997	1.58	Ribonuclease III, nuclear
H95348	Hs.159437	2.31	Transcribed locus, strongly similar to NP 002754.2 prospero-related homeobox 1 (*Homo sapiens*)
H10192	Hs.594542	2.06	Transcribed locus
T79127	Hs.486228	3.07	Hypothetical protein LOC643749
AA938900	Hs.403857	2.03	Lymphocyte antigen 9
AI122680	Hs.314263	7.25	Bromodomain adjacent to zinc finger domain, 2A
AA683077	Hs.431850	2.04	Mitogen-activated protein kinase 1
AA018457	Hs.420036	5.20	Glutamate decarboxylase 1 (brain, 67 kDa)
AI276134	Hs.2549	2.26	Adrenergic, beta-3 receptor
AA922903	Hs.466910	4.11	Cytidine deaminase
BG698959	Hs.489051	1.57	Six transmembrane epithelial antigen of the prostate 2
CB997906	Hs.632089	2.28	Exosome component 1
R37145	Hs.412587	3.84	RAD51 homologue C (*Saccharamyces cerevisiae*)
N50729	Hs.597002	2.13	Transcribed locus
N74161	Hs.29189	2.96	ATPase, Class VI, type 11A
AA621535	Hs.522895	2.67	Ras association (RaIGDS/AF-6) domain family 4
AA427621	Hs.632728	1.69	Transmembrane protein 19

[a] Unigene (UG) cluster.

CHEMISTRY
AN ASIAN JOURNAL

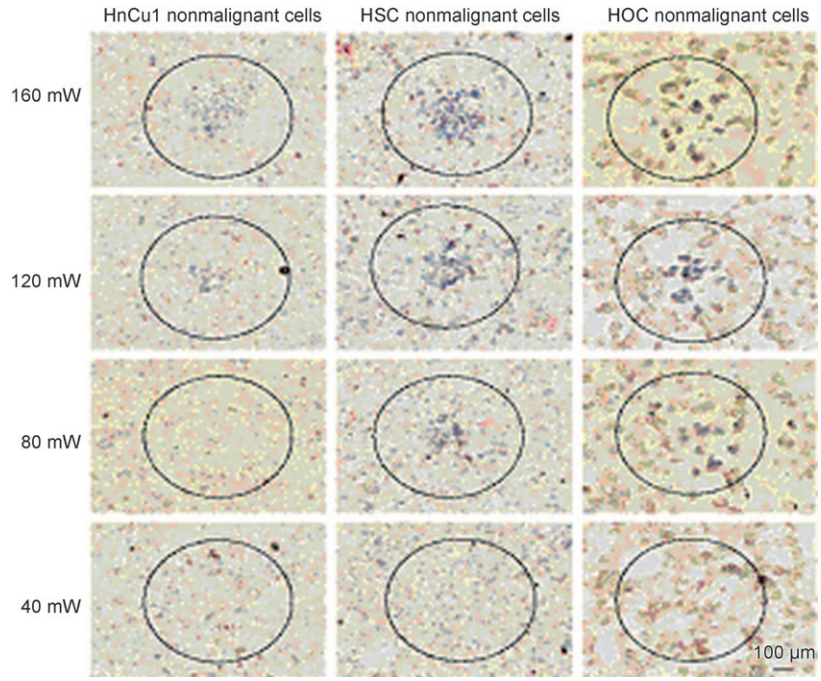

Figure 6. Selective photothermal therapy of cancer cells with anti-EGFR/GNRs incubated. The circles show the laser spots on the samples. The HSC and HOC malignant cells are obviously injured while the HaCat normal cells are not affected at 80 mW (10 $W cm^{-2}$). The HaCat normal cells start to be injured at 120 mW (15 $W cm^{-2}$) and are obviously injured at 160 mW (20 $W cm^{-2}$). Reprinted with permission from reference [26].

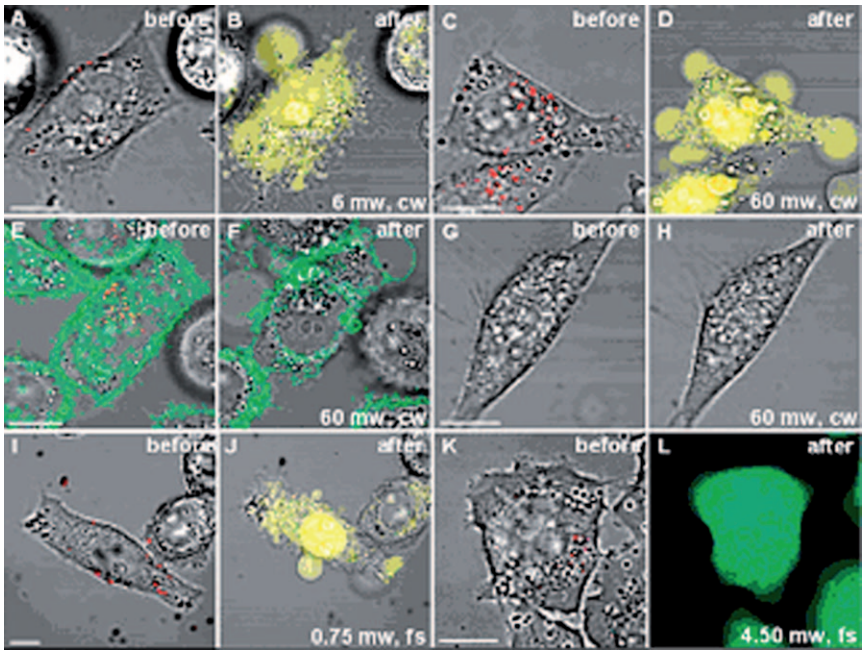

Figure 7. Site-dependent photothermolysis mediated by folate-GNRs (red). A,B) Cells with membrane-bound folate-GNRs exposed to cw NIR laser irradiation experienced membrane perforation and blebbing at 6 mW. The loss of membrane integrity was indicated by EB staining (yellow). C,D) At 60 mW. E,F) Folate-GNRs internalized in KB cells labeled by folate-bodipy (green) were exposed to laser irradiation at 60 mW, resulting in both membrane blebbing and melting of the folate-GNRs. G,H) NIH-3T3 cells did not suffer photoinduced damage upon 60 mW laser irradiation. I,J) Cells with membrane-bound folate-NRs exposed to fs-pulsed laser irradiation produced membrane blebbing. K,L) Cells with internalized folate-GNRs remained viable after fs-pulsed irradiation.Reprinted with permission from reference [99].

Nanomaterals may represent the chance to realize this goal. GNRs have several marked advantages such as enhanced scattering signal, no occurrence of photobleaching, and tunable longitudinal plasmon absorption, which can be used in multimodal contrast agents. GNRs exhibit highly efficient single- and two-photon-induced luminescence,[103] which attribute to their ability to keep resonating surface plasmons with minimal damping.[104] Owing to the strong scattering of light from GNRs, El-Sayed et al.[105] used a laboratory dark-field microscope to clearly visualize and distinguish the malignant cells from the nonmalignant cells. GNRs can aslo simultaneously serve as multimodal contrast agents for optical and electron microscopic imaging. Prasad et al.[102] combined dark-field imaging as well as electron microscopy imaging to study the uptake and orientation of targeted GNRs in vitro HeLa cell lines (Figure 8).

Cheng et al.[103] first reported the two-photon luminescence imaging of single GNRs. They found that TPL intensities from single GNRs are many times brighter than the TPL intensities from a single rhodamine molecule and demonstrated a $\cos^4$ dependence on excitation polarization. They monitored the flow of single GNRs using TPL through mouse ear blood vessels in vivo (Figure 9).

Ben-Yakar and co-workers[10] explored deep-tissue imaging utilizing TPL of GNRs. In contrast, the TPL intensity from GNR-labeled cancer cells is three orders of magnitude brighter than the two-photon autofluorescence emission intensity from unlabeled cancer cells.

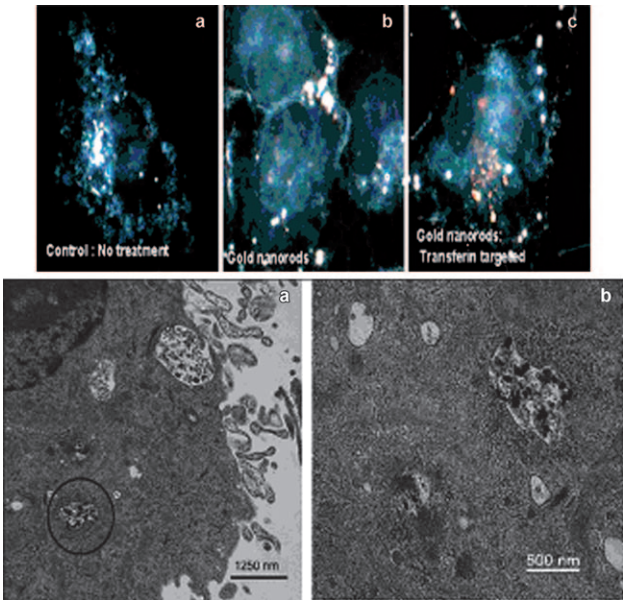

Figure 8. Top: Dark-field images of HeLa cells following a) no treatment, b) treatment with non-Tf-conjugated GNRs, and c) treatment with Tf-conjugated GNRs. The orange/red scattering corresponding to the GNRs, as seen in (c), originates from the strong longitudinal surface plasmon oscillation of the GNRs. Bottom: a) TEM image of HeLa cells with Tf-AuMLPs NRs (the circle points out GNRs). b) The circle in part (a) is magnified, showing the individual GNRs inside the cell cytoplasm. Reprinted with permission from reference [102].

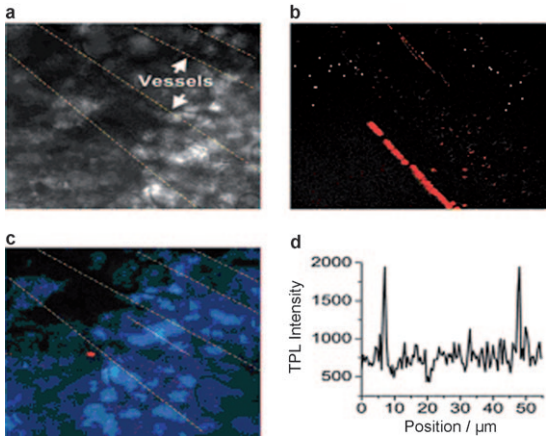

Figure 9. Imaging of single GNRs in mouse ear blood vessels in vivo. a) Transmission image with the two blood vessels indicated. Dotted contour lines are provided to guide the eye. b) TPL image of GNRs (red dots) flowing through the blood vessels. The bright signal beneath the lower blood vessel is the autofluorescence from a hair root. The streaking is due to sample drift during imaging. c) Overlay of the transmission image (light blue) and a single-frame TPL image. Two single nanorods (red spots) are superimposed by a linescan (white). d) TPL intensity profile from the linescan in (c). The background is due to autofluorescence from the blood vessel and the surrounding tissue. The similar intensities of the red spots indicate the detection of single GNRs. Reprinted with permission from reference [103].

6.3. Biosensing

Utilizing GNRs for biosensing has been reported. GNRs are sensitive to the dielectric constant of the surrounding medium owing to surface plasmon resonance. Therefore, a slight change of the local refractive index around GNRs will result in an observable shift of plasmon resonance frequency. Yu and Irudayaraj[9] fabricated GNRs of different aspect ratios with targeted antibodies to detect three targets (goat antihuman IgG1 Fab, rabbit antimouse IgG1 Fab, rabbit antisheep IgG (H+L)). In this study, they showed that GNRs can be used for a multiplexing detection device of various targets. Then, they designed and fabricated multiplex GNRs probes to identify up to three cell surface markers simultaneously with the aid of dark-field microscopy integrated with a special image system. In another study, they examined the quantification of the plasmonic binding events and estimation of ligand-binding kinetics for ligands tethered to GNRs by building up a mathematical method.[106] The GNR-based sensors were found to be highly specific and sensitive with the dynamic response in the range 10^{-9} to 10^{-6} M. For higher-target affinity pairs, one can expect to reach the femtomolar levels of detection, which is promising for developing sensitive and precise sensors for biological molecular interactions. Chilkoti and co-workers miniaturized[107] the biosensors to the dimensions of a single gold nanorod. Based on the proof-of-concept experiment of streptavidin and biotin, they tracked the wavelength shift using a dark-field microspectroscopy system. GNRs bound with 1 nM streptavidin could cause a 0.59 nm mean wavelength shift. Furthermore, they also indicated that the optical setup could reliably measure wavelength shifts as small as 0.3 nm. Using the fluorescence properties of long-aspect-ratio GNRs (aspect ratio > 13), Luong et al.[108] exploited GNRs as a novel sensitive probe for DNA hybridization. Interestingly, recently Frasch and co-workers have set single-molecule DNA detection in spin by linking F_1-ATPase motors and GNRs (Figure 10).

The biosensing nanodevice overcomes the defects inherent to polymerase chain reaction (PCR) or ligase chain reaction (LCR), is faster, and reaches zeptomole concentrations (600 DNA molecules), which is greatly superior to traditional fluorescence-based DNA detection systems which have detection limits of only about 5 picomolar. At present, nanoparticle-based surface-enhanced Raman tags have gained much attention as a valuable tool for ultrasensitive detection for biological cells.[109,110] GNRs are thought to be attractive candidates for SERS.[111] El-Sayed et al.[105] found that cancers cells assembled and aligned anti-EGFR/GNRs homogeneously owing to the overexpression of EGFR on the cancer cell surface. Molecules near the GNRs on the cancer cells give a greatly enhanced, sharp, and polarized Raman spectrum and can be used as diagnostic signatures for cancer cells. Ma and co-workers[28] prepared a composite material which is composed of GNR-embedded silica particles and organic Raman molecules as Raman label. In an immunoassay, the novel Raman label showed potential use for multiplex and ultrasensitive detection of biomolecules. Additionally, some groups also utilized functionalized GNRs as chemical sensors to detect Hg^{II},[112] Fe^{II},[113] and other ions.

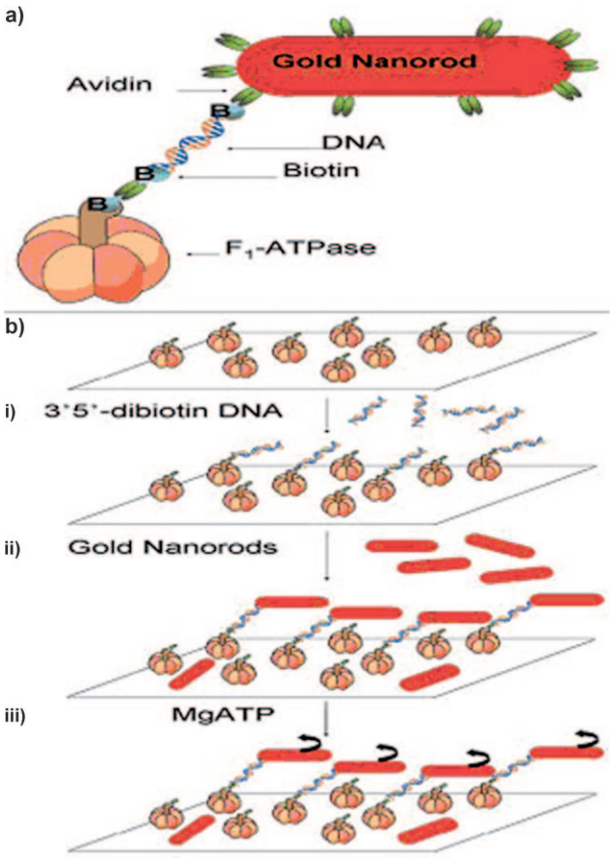

Figure 10. Self-assembly of the single-molecule biosensing device. a) Components of the nanodevice include: F_1-ATPase biomolecular motor modified to contain a 6xHis tag on each a subunit for immobilization to a Ni-NTA-coated slide; a biotinylated c subunit bound to avidin; the target-dependent 3′,5′-dibiotinylated DNA bridge; and an avidin-coated 80×30 nm gold nanorod. b) Sequential steps in nanodevice assembly: i) Binding of 3′,5′-dibiotinylated-DNA bridges to immobilized avidinated F_1-ATPase; ii) avidin-coated gold nanorod binding to immobilized DNA bridges; iii) Mg^{2+}-ATP-dependent rotation of nanorods for positive identification of the presence of target DNA. Reprinted with permission from reference [108].

6.4. Gene Delivery

The use of nanomaterials such as dendrimers, liposomes, magnetic nanoparticles, and carbon nanotubes for gene delivery has been of great interest.[114–117] GNRs, an emerging nanomaterial with anisotropic and rod-shaped characteristics, are attracting much attention in the field of gene delivery. Leong and co-workers[13] fabricated bifunctional Au/Ni nanorods through a template synthesis. Plasmids are bound to the Ni rod part while transferrin is bound to the Au rod part (Figure 11).

Although their transfection experiments in vitro and in vivo provided promising applications in genetic vaccination, the synthesis method is subtle and the yield is low. It is interesting that a pulsed NIR laser can induce the shape change of GNRs from rod to spherical and enhance the localized gene expression efficiency greatly. Yamada and co-workers[118] have examined the controlled release of plasma DNA from PC-capped GNRs. When a pulsed NIR laser irradiated the PC-GNR-DNA complexes, morphological change[119] occurred from rod into spherical. During this process, binding plasma DNA was released. Since PC-capped GNRs are not well-dispersed, recently the group has adopted a layer-by-layer technique to study GNR gene delivery.[66] The surface of the GNRs was modified with bovine serum (BSA),[116] which enhanced stabilization, and polyethylenimine (PEI), which strengthened transfection efficiency. However, the transfection efficiency was lower than that of PEI/DNA complexes. Future work should be directed toward obtaining a "fine-tuned" surface for successful gene delivery.

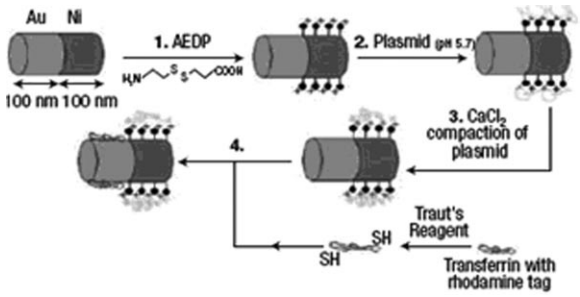

Figure 11. Schematic illustrations of multifunctional Au–Ni nanorods for gene delivery. Plasmids are bound by electrostatic interactions to the surface of the nickel segment. Rhodamine-conjugated transferrin is selectively bound to the gold segment of the nanorods. Reprinted with permission from reference [13].

Chen and co-workers[14] systematically examined near-infrared light-triggered release of DNA bonded to GNRs. They attached GNRs to the gene of enhanced green fluorescence protein (EGFP) for remote control of gene expression in living cells (Figure 12). DNA-SH was linked to the surface of GNRs through Au–S bonds. The resulting conjugates showed very good water solubility without precipitation or aggregation. When the conjugates were exposed to femtosecond NIR irradiation, the group also observed the same phenomenon, which was in agreement with Yamanda's observation[118] that GNRs changed their shapes and sizes(Figure 13). They proposed thermal and electron heating as two possible kinetic mechanisms to explain the Au–S bond cleavage. Owing to their IR-controllable character, GNRs have also some potential in exploring intelligent capsules[120,121] which can be triggered by exposure of light irradiation to open and release their contents.

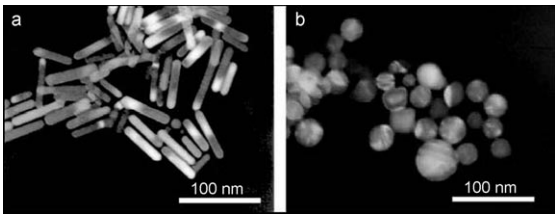

Figure 12. TEM images of the PC-GNRs before laser irradiation (rod; a) and the PC-NR-DNA complexes after laser irradiation with 1064 nm light (spherical; b). Reprinted with permission from reference [14].

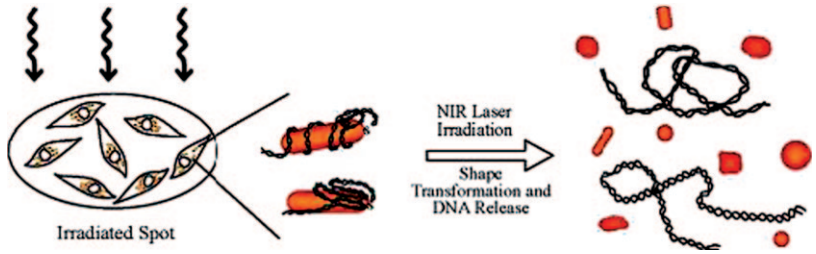

Figure 13. Schematic illustration of cells containing EGFP-GNR conjugates within a spot (3.5 mm in diameter) when irradiated by an NIR laser (left). After laser irradiation, EGFP-GNR conjugates undergo shape transformation that result in the release of EGFP-DNA (right). Reprinted with permission from reference [14].

7. Conclusions

GNRs have shown numerous desirable physical, chemical, electronic, and optical properties. Aside from other possible applications, currently, their biological applications are being widely and deeply pursued,[122] especially in photothermal therapy, molecular imaging, biosensing, and gene delivery. Compared with another important nanomaterial, CNTs (carbon nanotubes),[123,124] GNRs have raised less debate and concerns regarding their toxic nature. But this does not mean that this material is safe to human health and the environment in the long term. There are still extensive issues remaining to be addressed, for example, how to optimize the surface of GNRs elegantly to reduce CTAB negative effects, how to scale up GNRs to industrial production, and how to clearly elucidate the interaction mechanisms between GNRs and biological molecules, cells, and tissues as well as organs. So far, no groups have undertaken efforts to examine a detailed preclinical evaluation process referring to absorption, distribution, metabolism, excretion, and toxicity (ADMET) profiling. Future work needs to proceed along these lines before this material can be widely accepted in the public so that real biomedical application will be achieved as soon as possible.

Acknowledgements

The work is supported by China 973 project (No.2005CB724300-G), National Natural Science Foundation of China (No.20771075), 863 Project (No.2007AA022004), Shanghai Nano-progect (No.0752nm024), Shanghai Pujian Plan Project (No.06J14049), and Shanghai Foundation of Science and Technology (No.054119527). Prof. Ming-Yong Han (Institute of Materials Research and Engineering, Singapore National University) is appreciated for his helpful suggestions.

[1] N. Cioffi, L. Torsi, N. Ditaranto, G. Tantillo, L. Ghibelli, L. Sabbatini, T. Bleve-Zacheo, M. D′Alessio, P. G. Zambonin, E. Traversa, *Chem. Mater.* **2005**, *17*, 5255–5262.
[2] G. A. DeVries, M. Brunnbauer, Y. Hu, A. M. Jackson, B. Long, B. T. Neltner, O. Uzun, B. H. Wunsch, F. Stellacci, *Science* **2007**, *315*, 358–361.
[3] R. C. Jin, Y. W. Cao, C. A. Mirkin, K. L. Kelly, G. C. Schatz, J. G. Zheng, *Science* **2001**, *294*, 1901–1903.
[4] L. Y. Wang, J. W. Bai, Y. J. Li, Y. Huang, *Angew. Chem.* **2008**, *120*, 2473–2476; *Angew. Chem. Int. Ed.* **2008**, *47*, 2439–2442.
[5] X. H. Huang, P. K. Jain, I. H. El-Sayed, M. A. El-Sayed, *Nanomedicine* **2007**, *2*, 681–693.
[6] T. B. Huff, L. Tong, Y. Zhao, M. N. Hansen, J. X. Cheng, A. Wei, *Nanomedicine* **2007**, *2*, 125–132.
[7] X. Liu, Q. Dai, L. Austin, J. Coutts, G. Knowles, J. H. Zou, H. Chen, Q. Huo, *J. Am. Chem. Soc.* **2008**, *130*, 2780–2782.
[8] C. D. Chen, S. F. Cheng, L. K. Chau, C. R. C. Wang, *Biosens. Bioelectron.* **2007**, *22*, 926–932.
[9] C. X. Yu, J. Irudayaraj, *Anal. Chem.* **2007**, *79*, 572–579.
[10] N. J. Durr, T. Larson, D. K. Smith, B. A. Korgel, K. Sokolov, A. Ben-Yakar, *Nano Lett.* **2007**, *7*, 941–945.
[11] K. Imura, T. Nagahara, H. Okamoto, *J. Chem. Phys.* **2005**, *122*. 154701–154705.
[12] K. Imura, T. Nagahara, H. Okamoto, *J. Phys. Chem. B* **2005**, *109*, 13214–13220.
[13] A. K. Salem, P. C. Searson, K. W. Leong, *Nat. Mater.* **2003**, *2*, 668–671.
[14] C. C. Chen, Y. P. Lin, C. W. Wang, H. C. Tzeng, C. H. Wu, Y. C. Chen, C. P. Chen, L. C. Chen, Y. C. Wu, *J. Am. Chem. Soc.* **2006**, *128*, 3709–3715.
[15] A. Bouhelier, M. R. Beversluis, L. Novotny, *Appl. Phys. Lett.* **2003**, *83*, 5041–5043.
[16] A. Bouhelier, J. Renger, M. R. Beversluis, L. Novotny, *J. Microsc.* **2003**, *210*, 220–224.
[17] N. R. Jana, L. Gearheart, C. J. Murphy, *J. Phys. Chem. B* **2001**, *105*, 4065–4067.
[18] J. Perez-Juste, I. Pastoriza-Santos, L. M. Liz-Marzan, P. Mulvaney, *Coord. Chem. Rev.* **2005**, *249*, 1870–1901.
[19] S. Link, M. A. El-Sayed, *J. Phys. Chem. B.* **1999**, *103*, 8410–8426.
[20] O. P. Varnavski, M. B. Mohamed, M. A. El-Sayed, T. Goodson, *J. Phys. Chem. B.* **2003**, *107*, 3101–3104.
[21] K. Imura, T. Nagahara, H. Okamoto, *J. Am. Chem. Soc.* **2004**, *126*, 12730–12731.
[22] R. Weissleder, *Nat. Biotechnol.* **2001**, *19*, 316–317.
[23] D. E. J. G. J. Dolmans, D. Fukumura, R. K. Jain, *Nat. Rev. Cancer* **2003**, *3*, 380–387.
[24] S. E. Singletary, B. D. Fornage, N. Sneige, M. I. Ross, R. Simmons, A. Giuliano, N. Hansen, H. M. Kuerer, L. A. Newman, F. C. Ames, G. Babiera, F. Meric, K. K. Hunt, B. Edeiken, A. N. Mirza, *Cancer J.* **2002**, *8*, 177–180.
[25] A. N. Mirza, B. D. Fornage, N. Sneige, H. M. Kuerer, L. A. Newman, F. C. Ames, S. E. Singletary, *Cancer J.* **2001**, *7*, 95–101.
[26] X. H. Huang, I. H. El-Sayed, W. Qian, M. A. El-Sayed, *J. Am. Chem. Soc.* **2006**, *128*, 2115–2120.
[27] B. Nikoobakht, M. A. El-Sayed, *J. Phys. Chem. A* **2003**, *107*, 3372–3378.
[28] C. G. Wang, Y. Chen, T. T. Wang, Z. F. Ma, Z. M. Su, *Adv. Funct. Mater.* **2008**, *18*, 355–361.
[29] A. Gulati, H. Liao, J. H. Hafner, *J. Phys. Chem. B* **2006**, *110*, 22323–22327.
[30] A. Gole, C. J. Murphy, *Chem. Mater.* **2004**, *16*, 3633–3640.
[31] T. S. Hauck, A. A. Ghazani, W. C. W. Chan, *Small* **2008**, *4*, 153–159.
[32] A. R. Tao, S. Habas, P. D. Yang, *Small* **2008**, *4*, 310–325.
[33] A. B. Smetana, J. S. Wang, J. Boeckl, G. J. Brown, C. M. Wai, *Langmuir* **2007**, *23*, 10429–10432.
[34] N. Zhao, Y. Wei, N. J. Sun, Q. J. Chen, J. W. Bai, L. P. Zhou, Y. Qin, M. X. Li, L. M. Qi, *Langmuir* **2008**, *24*, 991–998.
[35] J. Y. Chen, B. Wiley, Z. Y. Li, D. Campbell, F. Saeki, H. Cang, L. Au, J. Lee, X. D. Li, Y. N. Xia, *Adv. Mater.* **2005**, *17*, 2255–2261.
[36] S. E. Skrabalak, L. Au, X. D. Li, Y. Xia, *Nat. Protoc.* **2007**, *2*, 2182–2190.

[37] J. E. Millstone, G. S. Metraux, C. A. Mirkin, *Adv. Funct. Mater.* **2006**, *16*, 1209–1214.
[38] F. Hao, C. L. Nehl, J. H. Hafner, P. Nordlander, *Nano Lett.* **2007**, *7*, 729–732.
[39] P. S. Kumar, I. Pastoriza-Santos, B. Rodriguez-Gonzalez, F. J. Garcia de Abajo, L. M. Liz-Marzan, *Nanotechnology* **2008**, *19*, 015606.
[40] N. R. Jana, *Small* **2005**, *1*, 875–882.
[41] B. D. Busbee, S. O. Obare, C. J. Murphy, *Adv. Mater.* **2003**, *15*, 414–417.
[42] H. Y. Wu, W. L. Huang, M. H. Huang, *Cryst. Growth Des.* **2007**, *7*, 831–835.
[43] P. K. Jain, M. A. El-Sayed, *J. Phys. Chem. C.* **2008**, *112*, 4954–4960.
[44] C. H. Su, H. S. Sheu, C. Y. Lin, C. C. Huang, Y. W. Lo, Y. C. Pu, J. C. Weng, D. B. Shieh, J. H. Chen, C. S. Yeh, *J. Am. Chem. Soc.* **2007**, *129*, 2139–2146.
[45] J. Perez-Juste, L. M. Liz-Marzan, S. Carnie, D. Y. C. Chan, P. Mulvaney, *Adv. Funct. Mater.* **2004**, *14*, 571–579.
[46] F. Kim, J. H. Song, P. D. Yang, *J. Am. Chem. Soc.* **2002**, *124*, 14316–14317.
[47] C. J. Johnson, E. Dujardin, S. A. Davis, C. J. Murphy, S. Mann, *J. Mater. Chem.* **2002**, *12*, 1765–1770.
[48] D. K. Smith, B. A. Korgel, *Langmuir* **2008**, *24*, 644–649.
[49] C. G. Wang, T. T. Wang, Z. F. Ma, Z. M. Su, *Nanotechnology* **2005**, *16*, 2555–2560.
[50] H. J. Park, C. S. Ah, W. J. Kim, I. S. Choi, K. P. Lee, W. S. Yun, *J. Vac. Sci. Technol. A* **2006**, *24*, 1323–1326.
[51] C. J. Murphy, T. K. Sau, A. M. Gole, C. J. Orendorff, J. X. Gao, L. F. Gou, S. E. Hunyadi, T. Li, *J. Phys. Chem. B.* **2005**, *109*, 13857–13870.
[52] C. J. Murphy, A. M. Gole, S. E. Hunyadi, C. J. Orendorff, *Inorg. Chem.* **2006**, *45*, 7544–7554.
[53] T. K. Sau, C. J. Murphy, *Langmuir* **2004**, *20*, 6414–6420.
[54] N. Nath, A. Chilkoti, *J. Fluoresc.* **2004**, *14*, 377–389.
[55] G. Raschke, S. Brogl, A. S. Susha, A. L. Rogach, T. A. Klar, J. Feldmann, B. Fieres, N. Petkov, T. Bein, A. Nichtl, K. Kurzinger, *Nano Lett.* **2004**, *4*, 1853–1857.
[56] G. Raschke, S. Kowarik, T. Franzl, C. Sonnichsen, T. A. Klar, J. Feldmann, A. Nichtl, K. Kurzinger, *Nano Lett.* **2003**, *3*, 935–938.
[57] J. X. Gao, C. M. Bender, C. J. Murphy, *Langmuir* **2003**, *19*, 9065–9070.
[58] C. X. Yu, L. Varghese, J. Irudayaraj, *Langmuir* **2007**, *23*, 9114–9119.
[59] H. Takahashi, Y. Niidome, T. Niidome, K. Kaneko, H. Kawasaki, S. Yamada, *Langmuir* **2006**, *22*, 2–5.
[60] A. Gole, C. J. Murphy, *Chem. Mater.* **2005**, *17*, 1325–1330.
[61] J. W. Hotchkiss, A. B. Lowe, S. G. Boyes, *Chem. Mater.* **2007**, *19*, 6–13.
[62] T. Niidome, M. Yamagata, Y. Okamoto, Y. Akiyama, H. Takahashi, T. Kawano, Y. Katayama, Y. Niidome, *J. Controlled Release* **2006**, *114*, 343–347.
[63] I. Pastoriza-Santos, J. Perez-Juste, L. M. Liz-Marzan, *Chem. Mater.* **2006**, *18*, 2465–2467.
[64] Y. Niidome, K. Honda, K. Higashimoto, H. Kawazumi, S. Yamada, N. Nakashima, Y. Sasaki, Y. Ishida, J. Kikuchi, *Chem. Commun.* **2007**, *36*, 3777–3779.
[65] C. S. T. Laicer, T. Q. Chastek, T. P. Lodge, T. A. Taton, *Macromolecules* **2005**, *38*, 9749–9756.
[66] H. Takahashi, T. Niidome, T. Kawano, S. Yamada, Y. Niidome, *J. Nanopart. Res.* **2008**, *10*, 221–228.
[67] L. M. Liz-Marzán, M. Giersig, P. Mulvaney, *Langmuir* **1996**, *12*, 4329–4335.
[68] P. A. Buining, B. M. Humbel, A. P. Philipse, A. J. Verkleij, *Langmuir* **1997**, *13*, 3921–3926.
[69] R. K. Iler, *J. Colloid Interface Sci.* **1972**, *38*, 496–501.
[70] S. H. Liu, M. Y. Han, *Adv. Funct. Mater.* **2005**, *15*, 961–967.
[71] Y. Lu, Y. Yin, B. T. Mayers, Y. Xia, *Nano Lett.* **2002**, *2*, 183–186.
[72] S. H. Liu, Z. H. Zhang, M. Y. Han, *Anal. Chem.* **2005**, *77*, 2595–2600.
[73] D. K. Yi, S. T. Selvan, S. S. Lee, G. C. Papaefthymiou, D. Kundaliya, J. Y. Ying, *J. Am. Chem. Soc.* **2005**, *127*, 4990–4991.
[74] S. O. Obare, N. R. Jana, C. J. Murphy, *Nano Lett.* **2001**, *1*, 601–603.
[75] C. G. Wang, Z. F. Ma, T. T. Wang, Z. M. Su, *Adv. Funct. Mater.* **2006**, *16*, 1673–1678.
[76] J. Y. Chang, H. M. Wu, H. Chen, Y. C. Ling, W. H. Tan, *Chem. Commun.* **2005**, *8*, 1092–1094.
[77] B. Nikoobakht, Z. L. Wang, M. A. El-Sayed, *J. Phys. Chem. B.* **2000**, *104*, 8635–8640.
[78] B. P. Khanal, E. R. Zubarev, *Angew. Chem.* **2007**, *119*, 2245–2248; *Angew. Chem. Int. Ed.* **2007**, *46*, 2195–2198.
[79] K. K. Caswell, J. N. Wilson, U. H. F. Bunz, C. J. Murphy, *J. Am. Chem. Soc.* **2003**, *125*, 13914–13915.
[80] A. Gole, C. J. Murphy, *Langmuir* **2005**, *21*, 10756–10762.
[81] B. F. Pan, L. M. Ao, F. Gao, H. Y. Tian, R. He, D. X. Cui, *Nanotechnology* **2005**, *16*, 1776–1780.
[82] X. S. Kou, S. Z. Zhang, Z. Yang, C. K. Tsung, G. D. Stucky, L. D. Sun, J. F. Wang, C. H. Yan, *J. Am. Chem. Soc.* **2007**, *129*, 6402–6404.
[83] S. Z. Zhang, X. S. Kou, Z. Yang, Q. H. Shi, G. D. Stucky, L. D. Sun, J. F. Wang, C. H. Yan, *Chem. Commun.* **2007**, *18*, 1816–1818.
[84] X. G. Hu, W. L. Cheng, T. Wang, E. K. Wang, S. J. Dong, *Nanotechnology* **2005**, *16*, 2164–2169.
[85] H. L. Han, C. G. Wang, Z. F. Ma, Z. M. Su, *Nanotechnology* **2006**, *17*, 5163–5166.
[86] X. Y. Wang, Y. G. Kim, C. Drew, B. C. Ku, J. Kumar, L. A. Samuelson, *Nano Lett.* **2004**, *4*, 331–334.
[87] J. Kolny, A. Kornowski, H. Weller, *Nano Lett.* **2002**, *2*, 361–364.
[88] M. A. Correa-Duarte, J. Perez-Juste, A. Sanchez-Iglesias, M. Giersig, L. M. Liz-Marzan, *Angew. Chem.* **2005**, *117*, 4449–4452; *Angew. Chem. Int. Ed.* **2005**, *44*, 4375–4378.
[89] A. Gole, C. J. Orendorff, C. J. Murphy, *Langmuir* **2004**, *20*, 7117–7122.
[90] B. F. Pan, D. X. Cui, C. G. Ozkan, P. Xu, T. Huang, Q. Li, H. Chen, F. T. Liu, F. Gao, R. He, *J. Phys. Chem. C.* **2007**, *111*, 12572–12576.
[91] E. Dujardin, L. B. Hsin, C. R. C. Wang, S. Mann, *Chem. Commun.* **2001**, *14*, 1264–1265.
[92] Z. H. Nie, D. Fava, M. Rubinstein, E. Kumacheva, *J. Am. Chem. Soc.* **2008**, *130*, 3683–3689.
[93] T. B. Huff, M. N. Hansen, Y. Zhao, J. X. Cheng, A. Wei, *Langmuir* **2007**, *23*, 1596–1599.
[94] E. E. Connor, J. Mwamuka, A. Gole, C. J. Murphy, M. D. Wyatt, *Small* **2005**, *1*, 325–327.
[95] B. D. Chithrani, A. A. Ghazani, W. C. W. Chan, *Nano Lett.* **2006**, *6*, 662–668.
[96] B. D. Chithrani, W. C. W. Chan, *Nano Lett.* **2007**, *7*, 1542–1550.
[97] H. Takahashi, T. Niidome, A. Nariai, Y. Niidome, S. Yamada, *Nanotechnology* **2006**, *17*, 4431–4435.
[98] A. K. Oyelere, P. C. Chen, X. H. Huang, I. H. El-Sayed, M. A. El-Sayed, *Bioconjugate Chem.* **2007**, *18*, 1490–1497.
[99] L. Tong, Y. Zhao, T. B. Huff, M. N. Hansen, A. Wei, J. X. Cheng, *Adv. Mater.* **2007**, *19*, 3136–3141.
[100] R. S. Norman, J. W. Stone, A. Gole, C. J. Murphy, T. L. Sabo-Attwood, *Nano Lett.* **2008**, *8*, 302–306.
[101] D. Pissuwan, S. M. Valenzuela, C. M. Miller, M. B. Cortie, *Nano Lett.* **2007**, *7*, 3808–3812.
[102] H. Ding, K. T. Yong, I. Roy, H. E. Pudavar, W. C. Law, E. J. Bergey, P. N. Prasad, *J. Phys. Chem. C.* **2007**, *111*, 12552–12557.
[103] H. F. Wang, T. B. Huff, D. A. Zweifel, W. He, P. S. Low, A. Wei, J. X. Cheng, *Proc. Natl. Acad. Sci. USA* **2005**, *102*, 15752–15756.
[104] C. Sonnichsen, T. Franzl, T. Wilk, G. von Plessen, J. Feldmann, O. Wilson, P. Mulvaney, *Phys. Rev. Lett.* **2002**, *88*,077402–077404.
[105] X. H. Huang, I. H. El-Sayed, W. Qian, M. A. El-Sayed, *Nano Lett.* **2007**, *7*, 1591–1597.
[106] C. Yu, J. Irudayaraj, *Biophys. J.* **2007**, *93*, 3684–3692.
[107] G. J. Nusz, S. M. Marinakos, A. C. Curry, A. Dahlin, F. Höök, A. Wax, A. Chilkoti, *Anal. Chem.* **2008**, *80*, 984–989.
[108] C. Z. Li, K. B. Male, S. Hrapovic, J. H. T. Luong, *Chem. Commun.* **2005**, *31*, 3924–3926.

[109] X. M. Qian, X. H. Peng, D. O. Ansari, Q. Q. Yin-Goen, G. Z. Chen, D. M. Shin, L. Yang, A. N. Yong, M. D. Wang, S. M. Nie, *Nat. Biotechnol.* **2008**, *26*, 83–90.
[110] J. H. Kim, J. S. Kim, H. Choi, S. M. Lee, B. H. Jun, K. N. Yu, E. Kuk, Y. K. Kim, D. H. Jeong, M. H. Cho, Y. S. Lee, *Anal. Chem.* **2006**, *78*, 6967–6973.
[111] E. Hao, G. C. Schatz, *Jounal of Chemical Physics* **2004**, *120*, 357–366.
[112] C. C. Huang, H. T. Chang, *Anal. Chem.* **2006**, *78*, 8332–8338.
[113] J. J. Zhang, Y. G. Liu, L. P. Jiang, J. J. Zhu, *Electrochem. Commun.* **2008**, *10*, 355–358.
[114] B. Pan, D. Cui, Y. Shen, C. S. Ozkan, F. Gao, R. He, Q. Li, P. Xu, T. Huang, *Cancer Res.* **2007**, *67*, 8156–8164.
[115] D. Cui, F. Tian, S. R. Coyer, J Wang, F Gao, R. He, B. Pan and Y. Zhang, *J. Nanosci. Nanotechnol.* **2007**, *7*, 1639–1642.
[116] I. J. Majoros, A. Myc, T. Thomas, C. B. Mehta, J. R. Baker, *Biomacromolecules* **2006**, *7*, 572–574.
[117] D. Cui, *J. Nanosci. Nanotechnol.* **2007**, *7*, 1298–1234.
[118] H. Takahashi, Y. Niidome, S. Yamada, *Chem. Commun.* **2005**, *17*, 2247–2249.
[119] Y. Niidome, K. Nishioka, H. Kawasaki, S. Yamada, *Colloids and Surfaces A: Physicochemical and Engineering Aspects* **2005**, *257–258*, 161–164.
[120] B. F. Pan, D. X. Cui, P. Xu, Q. Li, T. Huang, R. He, F. Gao, *Colloids and Surfaces A: Physicochemical and Engineering Aspects.* **2007**, *295*, 217–222.
[121] E. Piskin, S. Dincer, M. Turk, *J. Biomater. Sci. Polym. Ed.* **2004**, *15*, 1181–1202.
[122] G. Sukhorukov, A. Fery, H. Mohwald, *Prog. Polym. Sci.* **2005**, *30*, 885–897.
[123] C. J. Murphy, A. M. Gole, S. E. Hunyadi, J. W. Stone, P. N. Sisco, A. Alkilany, B. E. Kinard, P. Hankins, *Chem. Commun.* **2008**, *5*, 544–557.
[124] G. Pagona, N. Tagmatarchis, *Curr. Med. Chem.* **2006**, *13*, 1789–1798.
[125] A. Bianco, M. Prato, *Adv. Mater.* **2003**, *15*, 1765–1768.

Received: May 5, 2008
Revised: June 24, 2008
Published online: October 27, 2008

